Large Number Hexagonal Cavities Microfluidic Digital Chip for Gene Mutation Ultrasensitive Analysis in Lung Cancer

Fei Liu (susufei@sina.com)
The Army Medical University
Pan Feng
The second affiliated hospital of the army medical university
Mingjing Guo
The Second Affiliated Hospital of the army medical university
Gang Li
Chongqing University
Tengbao Xie
Chongqing University
Liqun Zhang
The Second Affiliated Hospital of the army medical university
Xiaoyun Pu
The Second Affiliated Hospital of the army medical university

Research

Keywords: microfluidic chip, dPCR, lung cancer, gene mutation, detection

Posted Date: December 12th, 2020

DOI: https://doi.org/10.21203/rs.3.rs-124277/v1

Abstract

Lung cancer is the highest incidence of malignant tumors in the world. Targeted therapy based on gene mutation detection including epidermal growth factor receptor (EGFR) gene mutation is one of the first-line treatments. In this work, took EGFR gene G719S mutation as a representative object, a large number hexagonal cavities microfluidic chip (LHMC) platform based on digital PCR (dPCR) for the absolute quantification of gene mutation in lung cancer was established. In this chip, 113,137 cavities chip was designed to increase the number of absolute quantitative, which was 2~5 times higher than the traditional one. The hexagonal shape of cavities elevates the filling rate and filling speed. A set of primers and probes for G719S with high sensitivity, high specificity and high reliability were designed and screened. Then the PCR parameters were optimized. The results demonstrated that the chip platform shows good performance. The minimum detection concentration of the gene mutant was 3.01 copies/μL, and a good correlation (Y= 0.725X- 0.581, R^2= 0.984) was noted between the measured value and the expected value. This chip possesses sensitively detect positive mutations in G719S and completely negative when detecting other substances. The developed LHMC-dPCR chip is a rapid and accurate gene mutation analysis platform, which has faster speed and lower price than classic detection methods, for instance, droplet dPCR, DNA sequencing method. Moreover, LHMC-dPCR is not limited by the number of nucleic acids and droplets and there is no need to estimate the nucleic acid concentration of the sample. This chip platform could also detect other gene mutations, for example, L858R, exon 19 deletions, in other tumors including lung cancer.

1. Introduction

Lung cancer is the most prevalent malignancy worldwide and the leading cause of cancer death (18.4% of all cancers) [1]. Epidermal growth factor receptor (EGFR) mutations in Asian women with lung adenocarcinoma who have never smoked are up to 60% [2, 3].Several studies have shown that non-small cell lung cancer tumors and lung adenocarcinoma patients with somatic mutations in EGFR have a good effect on tyrosine kinase inhibitors (TKIs), such as gefitinib, erlotinib, and lapatinib [4–10]. However, even with the same type or even the same subtype, the response of different patients to TKIs is not consistent, and the different content of mutant molecules may be an important reason for the different responses of TKIs. And patients with tumors with higher EGFR mutation “abundance” are more responsive to the same drug. Therefore, the classification heterogeneity of lung cancer and accurate quantification of gene mutations is the key to improve the efficacy of targeted therapy and achieve precision medical treatment of lung cancer.

DNA sequencing is a common method for detecting EGFR mutations in early studies, and this method is useful for identifying both known and new mutations [4, 11, 12]. However, since DNA sequencing can only detect mutation sequences that account for more than 30% of the total gene content [13], this is not useful for detecting EGFR mutations in only a small fraction of the EGFR mutant sequences in the body fluids. In previous studies, amplification refractory mutation system (ARMS) analysis has been applied to detect circulating EGFR mutations [14, 15]. However, the ARMS method can only be qualitative and

cannot measure the concentration of circulating mutations, and the sensitivity of the ARMS method to detect point mutations at low concentrations may be low when detecting a large number of background wild-type sequences. Detection and quantification of EGFR low-abundance mutations in tumor tissues are also valuable. Analysis of EGFR mutations in 22 lung adenocarcinoma specimens by large-scale parallel sequencing revealed that EGFR mutations may be highly heterogeneous in a single tumor sample, with some mutations present only within 10% of the total sequence [16]. At present, the importance of detecting low-abundance mutations in tumor tissues is unclear. This may be due to the low proportion of tumor cells in tissue samples or may indicate that the mutant allele exists only in a subset of tumor cells [2], the latter situation may occur during cancer evolution [16]. A recent report demonstrated the acquired resistant of double mutant G719S/T790M to gefitinib [17]. However, as a sensitive mutation and drug-resistant mutation site, G719S is rarely studied due to its low mutation rate, and there are few available detection reagents. Mutation detection for G719S on the market is often included in G719X together with G719A and G719C. For example, Super-ARMS kit of Edwards Biology, it is difficult to specifically detect G719S mutation alone. In this article, to preliminarily evaluate the feasibility and sensitivity of LHMC-dPCR, G719S, a target with less mutation abundance, and it has both characteristics of sensitivity and resistance to targeted drugs, was selected for determination.

dPCR technology is a new generation of nucleic acid absolute quantitative technology that can detect a single molecule. It has a very prominent advantage in detecting rare point mutations in wild-type sequence backgrounds, and its application has spanned a large number of DNA, RNA and epigenetic applications [18–24]. The method has high sensitivity and high accuracy, and the absolute number of target molecules can be detected as low as a single copy without reference genes and standard curves. Compared with real-time fluorescent quantitative PCR (Real-Time PCR), dPCR has the advantages of high sensitivity, absolute quantification, high tolerance to inhibitors, and single-molecule sequencing [25, 26]. dPCR technology can be divided into ddPCR and chip digital PCR (cdPCR). There are many commercial ddPCR products in the market, but the detection cost is high. Due to the immature development of chip technology, cdPCR is rarely used in clinical gene mutation detection. Based on this, to reduce the cost of dPCR detection and enrich cdPCR technology, LHMC-dPCR is established in this article. The chips in this article have been improved over 3 generations. In previous studies [27, 28], the specific structure and performance of the previous generations of chips have been verified many times. LHMC has more microcavity structures and more stable performance than before, as well as faster sample loading speed. By selecting the EGFR G719S mutation as the target, the application value and performance of the new chip are evaluated in this article for the first time.

2. Experiments

2.1 Reagents

Premix Ex Taq™ (Probe qPCR) and BSA were obtained from TaKaRa Biotechnology (Tokyo, Japan). The Nucleic acid extraction kit was purchased from Shanghai Biochip Co. (Shanghai, China).The van-clear environmental transparent agent was purchased from Wuhan Hongzi Biotechnology Co. (Wuhan, China).

The polydimethylsiloxane (PDMS) (Sylgard 184 kit) was purchased from Dow Corning (Midland, MI, USA). Triton X-100 was obtained from Sigma-Aldrich China (Shanghai, China). Dimethylsilicone oil was purchased from Aladdin (Shanghai, China). TE buffer was obtained from Beijing Solarbio Science & Technology Co. (Beijing, China).

The primers and probes of G719S and standard plasmids including G719S gene mutation, L858R gene mutation, Codon12 gene mutation and H19-1 gene mutation were synthesized by Sangon Biotech (Shanghai) Co. (Shanghai, China).

2.2 Apparatus

SLAN-96P Real-Time PCR system was purchased from Shanghai Hongshi Medical Technology Co. (Shanghai, China). Mastercycler nexus flat was obtained from Eppendorf (Hamburg, German). The Small vacuum plasma cleaning machine was purchased from Tonson Tech (Shenzhen, China). Nib900 inverted fluorescence microscope was purchased from Ningbo Yongxin Optical Co. (Ningbo, China). DS-Qi2 Monochrome Microscope Camera was obtained from Nikon Instruments (Tokyo, Japan).

2.3 Clinical samples

Six cases of formalin-fixed paraffin-embedded (FFPE) tissue samples were collected from lung cancer patients with EGFR G719X mutation confirmed by the AmoyDx gene detection kit (Xiamen, China) in the Second Affiliated Hospital of the Army Medical University (Chongqing, China) from January 2020 to October 2020, 10 pieces for each case.

Inclusion criteria: (1) Patients with primary lung cancer diagnosed by imaging and signs and symptoms; (2) ECG, blood routine, the function of the liver, kidney, and bone marrow were basically normal; (3) Informed consent of patients and their families.

Exclusion criteria: (1) Consciousness disorder, psychiatric; (2) Have other serious basic diseases, such as diabetes, hypertension, pulmonary heart disease, hyperthyroidism, etc.; (3) Pregnant or lactating women; (4) Unknown consent or refusal to sign informed consent.

2.4 G719S mutant standard plasmids preparation

The obtained G719S mutant plasmids were diluted with TE buffer to 3.01×10^0 copies/μL, 3.01×10^1 copies/μL, 3.01×10^2 copies/μL, 3.01×10^3 copies/μL, 3.01×10^4 copies/μL, 3.01×10^5 copies/μL, 3.01×10^6 copies/μL, 3.01×10^7 copies/μL with a 10-fold concentration gradient. The above plasmids diluted by 10-fold gradient were numbered 1–8 as the standard.

2.5 Lung cancer tissue nucleic acid extraction

Six cases of FFPE tissue samples were scraped gently from the slides into 1.5 mL EP tubes with surgical blades and centrifuged at 12,000 rpm for 2 min. 1 mL van-clear environmental transparent agent was added, vigorously whirled for 10 s, centrifuged at 12,000 rpm for 2 min, and discarded the supernatant. 1 mL absolute ethanol was added to a 1.5 mL centrifuge tube, whirlpool and mixed, centrifuged at

12,000 rpm for 2 min, and discarded the supernatant. The cap of the tube was opened and stored at room temperature for 10 minutes until the absolute ethanol in the tube was evaporated. Then, extraction experiments were carried out according to the instructions of the extraction kit. The 6 cases of samples were numbered F1-F6 for standby application.

2.6 PCR amplification

The exon 19 with 341 bp of EGFR containing the G719S mutation site was selected. And primer and probe were designed by Primer premier software version 5.0 (Premier Biosoft International, Palo Alto, CA) and the highest score pairs were chosen. The sequences of the designed primers and probes are listed in Table. 1. A total volume of 25 μL of PCR reaction system was prepared using Premix Ex Taq™ (Probe qPCR) reagents in the following proportions: 12.5 μL PreMix, 6.375 μL ddH2O, 0.625 μL BSA (20 mg/mL), 1 μL of each primer, 1 μL of probe and 2.5 μL template. The amplification conditions were as follows: (1) Pretreatment with 95 ℃, 30 s; (2) Amplified 45 cycles according to such parameters 95 ℃, 40 s, and 56 ℃, 40 s; (3) Heat preservation at 4 ℃.

Table 1
The sequences of the designed primers and probes

Sequence name	Sequence (5'- 3')	Modification
Forward primer	TGAGGATCTTGAAGGAAACTGA	
Reverse primer	CCTTATACACCGTGCCGAAC	
Mutant type probe	AAGTGCT + GGGCTC	5'-FAM, 3'-MGB
Wild type probe	AGTGCT + GAGCTCC	5'-HEX, 3'-MGB

2.7 Fabrication of LHMC

The fabrication process of LHMC is shown in Fig. 1A. Briefly, the specific process is as follows: (1) PDMS prepolymer, curing agent were mixed at a ratio of 10:1, which Triton X-100 was added into at final concentration with 0.5%, degassed for 30 min (Fig. 1Aa); (2) The PDMS/Triton X-100 mixture was poured onto the master molds and smoothly covered with a PET film. Glass sheet and weight were added above the PET film to form PDMS thin layer (~ 500 μm) and PDMS cover plate (~ 2 mm), and the PDMS was cured by heating at 70 ℃ for 1–3 h (Fig. 1Ab); (3) The weight and the covered glass plate were removed, peeled off the PET/PDMS layers from the master mold. The PDMS pipeline was punched in a specific position with a 2 mm puncher (Fig. 1Ac); (4) The unstructured surface of the PDMS thin layer with microcavity structure was bond to the clean glass slide through oxygen plasma treatment. Meanwhile, the structural surface of the PDMS thin layer was attached with the PDMS pipeline to form a reversible seal (Fig. 1Ad).

As schematically depicted in Fig. 1B, it consists of three layers: a 2-mm thickness PDMS pipeline as a detachable pumping source, a 500-μm PDMS thin layer as a digitally divided chamber, and a glass slide as a supporting layer. The PDMS pipeline contains 40 parallel microfluidic channels (Fig. 1C), and the

PDMS thin layer contains 113,137 regularly arranged microarrays (Fig. 1D). The structure of the pipeline layer is slightly larger than that of the film layer so that the sample can be digitally divided through the delivery channel. The depth of each cavity is 40 μm, and the distance between opposite sides is 60 μm.

2.8 LHMC-dPCR detection steps

The detection process of LHMC-dPCR is shown in Fig. 2. Firstly, the prepared LHMC was put into the vacuum pump and degassed for 20 minutes. Then 25 μl of the prepared PCR premix was added into the injection hole immediately, and stood for 5–30 s to realize the self-separation and self-distribution of the liquid sample in 113,137 microcavity arrays. After that, 200 μL dimethylsilicone oil was added and the PDMS pipeline was peeled off at the same time. Next, the oil seal chip was sealed by covering a glass slide covered with a thin layer of un-solidified PDMS. Then the sealed chip was placed on the mastercycler nexus flat for the amplification reaction. Finally, the amplified chip was observed by imaging with a fluorescence microscope.

2.9 Statistical processing

The number of positive holes in the chip was quantified through the counting function of ImageJ. According to previous studies [28], the theoretical formula applicable to LHMC can be obtained as follows:

$$C = -8000 \times \ln\left[1 - \frac{N_p}{113137}\right] \quad (1)$$

The formula for calculating sample concentration (C) has been derived by our collaborators according to the Poisson distribution formula:

$$C = \frac{\ln\left[1 - \frac{N_p}{n}\right]}{V_d} \quad (2)$$

Where Np is the number of positive partitions, n is the number of the micro-cavity, and Vd is the volume of each partition. The results of the calculation were further analyzed by OriginPro software version 8.0 (OriginLab Corporation, Northampton, MA, USA).

3. Results And Discussion

3.1 Chip imaging

All the images of bright field and fluorescent channel were taken by an inverted microscope. As shown in Fig. 3A, the result of a representative sample amplified in the LHMC was shown in a fluorescent micrograph: chambers that do not contain target DNA display low fluorescence levels (i.e., "negative signals"), while chambers that contain target DNA displayed high fluorescence levels (i.e., "positive signals"). After fluorescence imaging, ImageJ software version 1.53c (National Institutes of Health, Bethesda, Maryland) was used to analyze the images and quantify the number of positive cavities in each LHMC. As shown in Fig. 3B, the fluorescence of the representative sample was converted to a gray level in ImageJ. Then, as shown in Fig. 3C, the number of positive holes in the chip was quantified by ImageJ with two indicators of diameter and brightness.

The physical image of the LHMC is as shown in Fig. 3D. In this work, the entire chip is the size of a microscope slide (25 mm * 75 mm * 2.5 mm), and the air permeability of PDMS can be used to quickly fill the sample. Compared with the previous design of the chip, the improved chip has many more advantages than the former. Since the microcavity is redesigned as a regular hexagonal prism instead of a cylinder, on the microarrays of the same size as the previous ones, the microarrays in the thin film layer of the LHMC are composed of 5 times more microcavities. Besides, the pipelines connecting the microcavities were removed and designed in a detachable PDMS pipeline, so that the steps of oil flushing out excess samples were reduced. Besides, the sample adsorption is reduced and more positive holes are obtained by adding more appropriate Triton X-100 and BSA.

3.2 PCR amplification system establishment

Due to the detection limit of dPCR technology is affected by the end-point fluorescence value, it is necessary to optimize the annealing temperature and the concentration of primers and probes. In turn, the optimal reaction conditions will also increase the efficiency of the entire reaction. Therefore, the annealing temperature, the concentration of primer and probe, specificity and repeatability of the EGFR G719S amplification system were first optimized and verified outside the LHMC.

3.2.1 Optimization of annealing temperature

According to the amplification results (Fig. S1), in the designed EGFR G719S PCR system, the target gene was amplified correctly and the genotype was accurately identified within the range of 55–58 ℃, indicating that the specificity of the primers and probes is good. Moreover, the repeatability was the best at 56 ℃. Therefore, the optimal annealing temperature was determined to be 56 ℃.

3.2.2 Optimization of primer concentration

To determine the best primer concentration with the highest fluorescence value, a probe of 0.4 μM and a template of 2.5 μM were added at the optimal annealing temperature of 56 ℃ for PCR amplification. The experimental results showed (Fig. 4A) that the fluorescence value was proportional to the primer concentration in the range of 0.1–0.9 μM. Besides, the fluorescence value was the highest when the primer concentration was 0.9 μM and slightly decreased when the primer concentration was 1 μM. Therefore, 0.9 μM was determined as the optimal concentration of primer.

Similarly, to determine the optimal probe concentration with the highest fluorescence value, a template of 2.5 μM was added at the optimal annealing temperature of 56 ℃ and the optimal primer concentration of 0.9 μM for PCR amplification. The results show that within the concentration range of 0.1–0.5 μM, the relative fluorescence value of the amplification curve is inverse-proportional to the probe concentration (Fig. 4B), while the absolute fluorescence value of the original curve is proportional to the probe concentration (Fig. 4C). The trend of the amplified curve is opposite to that of the original curve because the more probes were added, the higher the background, the lower the relative increment. Therefore, to ensure the highest endpoint fluorescence value, 0.5 μM was determined as the optimal probe concentration.

3.2.3 Repeatability of PCR

According to the results of repeatability experiment (Fig. S2), the target gene in the current system has been accurately and repeatedly detected.

3.3 Performance of dPCR in LHMC

Figure 5A-H shows the fluorescence microscopy of the amplification results of the standard plasmids No. 1–8 detected by LHMC-dPCR. The positive partitions of mutant plasmids was significantly proportional to the concentration of the plasmids template in the PCR mixture. Furthermore, the relationship between the expected concentration value and the actual concentration value of the above linear plasmids was compared. Figure 5I shows the plot of the measured concentrations against their expected values. From the linear regression analysis, we obtain a high coefficient of determination ($R^2 = 0.984$) across a dynamic range of over 8 orders of magnitude, which reveals a close fit between the concentrations of measured and expected.

3.4 The detection sensitivity LHMC-dPCR

Different from the previous report, the number of LHMC increased from 20,000 to 113,137, and the Vd was updated to 0.125 nL. When there is only one positive partition, the minimum detection limit of the LHMC can be calculated as 0.070 copies/μL. However, due to the influence of many factors in practical nucleic acid testing, the minimum value of chip detection is often higher than the theoretical value. In our experiment, the sensitivity of LHMC was 3.01 copies/μL, which is much higher than DNA sequencing, qPCR and ARMS, *etc.*

3.5 Specificity for LHMC-PCR

To verify the anti-interference ability of the system on LHMC, we selected various types of substances for interference experiments 20.5 g/L albumin standard solution (the main substance in serum), 2.88×10^8 copies/μL H19-1 mutant plasmids (mutation of long non-coding RNA), 3.01×10^8 copies/μL Codon12 mutant plasmids, and 3.20×10^8 copies/μL L858R mutant plasmids (the other two mutations of EGFR) were determined separately. And then the above interfering substances were mixed with equal amounts of 3.01×10^5 copies/μL G719S mutant plasmids. The mixture and the same concentration of G719S standard plasmids were tested separately. As is shown in Fig. 6, the results showed that no positive

partition was found in 20.5 g/L albumin standard solution, 3.01×10^8 copies/μL Codon12 mutant plasmids, 3.20×10^8 copies/μL L858R mutant plasmids, and 2.88×10^8 copies/μL H19-1 mutant plasmids. Besides, the number of positive partitions in the mixture system is basically the same as that in the similarly diluted standard No. 6, indicating that the system has good specificity and strong anti-interference ability.

3.6 Application in clinical samples

Although tumor tissue is difficult to obtain, it is still the most used source of DNA templates for tumor genetic testing. Because in terms of gene mutations, especially for samples with low mutation abundance, the accuracy of mutation concentration detection results is often greatly affected due to the low mutation rate and sensitivity limitations of detection technology. To verify the application of LHMC-dPCR in actual clinical samples, LHMC-dPCR, DNA sequencing and ddPCR were used to detect FFPE tissue samples from 6 cases of lung cancer patients with EGFR G719X positive mutations to compare these methods.

The comparison of test results of LHMC-dPCR, DNA sequencing and ddPCR was shown (Table. 2). In the detection of LHMC-dPCR and ddPCR (Fig. S3, S4), positive samples can be observed quickly and intuitively, and the concentration of mutation can be roughly judged. In addition, the concentration of the mutant nucleic acid in the sample can be calculated by substituting the corresponding formula. However, as shown in Fig. S5, DNA sequencing can be used to compare and find the mutation sites, but the content of the mutated genes cannot be quantified.

Table 2
Comparison of the detection results of LHMC-dPCR, ddPCR, and DNA sequencing

Samples	Methods		
	DNA sequencing	ddPCR (copies/μL)	LHMC-dPCR (copies/μL)
F1	Q. (-)	0	0
F2	Q. (+)	1822.4	1581.8
F3	Q. (-)	0	0
F4	Q. (-)	0	0
F5	Q. (+)	218.3	451.7
F6	Q. (-)	0	0
Q.: only qualitative			

Moreover, in the actual detection process, the total number of droplets detected by ddPCR is limited. And to determine the appropriate sample volume that should be added, the total nucleic acid concentration of the sample usually needs to be measured before this. If the total nucleic acid concentration of the sample exceeds the total number of droplets, the sample needs to be diluted to different degrees before detection. Therefore, in addition to unnecessary errors caused by the increase in operating steps, the test results may also appear false negatives when the content of wild-type genes is far greater than the content of mutations. In contrast to this, the LHMC-dPCR we established can directly detect samples without other processing of nucleic acids, because the number of nucleic acids and the number of droplets does not affect the detection results of LHMC-dPCR. At the same time, LHMC can be made in batches in advance by copying many master models to save the entire inspection time.

4. Conclusions

In summary, the LHMC-dPCR established could achieve real-time and absolute quantitative detection for samples without standard curves and reference control genes. It has the advantages of low cost, simple operation, fast speed, strong anti-interference ability and high repeatability. According to the results, EGFR G719S could be accurately and quickly detected by LHMC-dPCR. And other gene mutations of lung cancer may also be accurately detected by LHMC-dPCR as long as specific probes and primers are designed. In our follow-up research, more gene mutations and even bacteria would be used in LHMC detection. The establishment of LHMC-dPCR not only enriches cdPCR technology but also provides another good choice for the clinical application and scientific research of other sample detection.

Abbreviations

EGFR: epidermal growth factor receptor. LHMC: large number hexagonal cavities microfluidic chip. dPCR: digital PCR. TKIs: tyrosine kinase inhibitors. ARMS: amplification refractory mutation system. Real-Time PCR: real-time fluorescent quantitative PCR. cdPCR: chip digital PCR. PDMS: polydimethylsiloxane. FFPE: formalin-fixed paraffin-embedded. PET: polyethylene terephthalate.

Declarations

Ethics approval and consent to participate

All protocols requiring the use of FFPE tissue samples collected from lung cancer patients were approved by The Medical Ethics Committee of the Second Affiliated Hospital, Army Medical University.

Availability of data and materials

The data and materials used and/or analyzed during the current study are available from the corresponding author on reasonable request.

Competing interests

The authors declare that they have no competing interests.

Consent for publication

Not applicable.

Authors' contributions

GL and XYP designed the structure of the LHMC. FL and LQZ participated in the design of this study. PF and TBX carried out the fabrication of the chip. MJG conducted the works of the extraction of tissue specimens. PF carried out the detection of LHMC-dPCR, processed data, and prepared the draft of the manuscript. FL revised the manuscript. All authors agreed on the final version of the paper.

Funding

This work was supported by the National Natural Science Foundation of China (No. 81772284), Top project of military medical science and technology youth training program (20QNPY029), Chongqing Technical Innovation and Application Demonstration Program (cstc2018jscx-mszdX0073), and Chongqing Technology Innovation and application development project (cstc2019jscx-msxmX0131).

Acknowledgements

We much appreciate the valuable comments that we received from other members of our laboratories.

References

1. Bray F, Ferlay J, Soerjomataram I, Siegel R L, Torre L A, Jemal A. Global cancer statistics 2018: GLOBOCAN estimates of incidence and mortality worldwide for 36 cancers in 185 countries. CA: A Cancer Journal for Clinicians. 2018;68:394-424.
2. Nagai Y, Miyazawa H, Huqun, Tanaka T, Udagawa K, Kato M, et al. Genetic Heterogeneity of the Epidermal Growth Factor Receptor in Non–Small Cell Lung Cancer Cell Lines Revealed by a Rapid and Sensitive Detection System, the Peptide Nucleic Acid-Locked Nucleic Acid PCR Clamp. Cancer Research. 2005;65:7276.
3. Shigematsu H, Gazdar A F. Somatic mutations of epidermal growth factor receptor signaling pathway in lung cancers. Int J Cancer. 2006;118:257-262.
4. Thomas J Lynch D W B, Raffaella Sordella, Sarada Gurubhagavatula, Ross A Okimoto, Brian W Brannigan, Patricia L Harris, Sara M Haserlat, Jeffrey G Supko, Frank G Haluska, David N Louis, David C Christiani, Jeff Settleman, Daniel A Haber. Activating mutations in the epidermal growth factor receptor underlying responsiveness of non-small-cell lung cancer to gefitinib. New England Journal of Medicine. 2004;350:2129–2139.

5. Paez J G, Jänne P A, Lee J C, Tracy S, Greulich H, Gabriel S, et al. EGFR Mutations in Lung Cancer: Correlation with Clinical Response to Gefitinib Therapy. Science. 2004;304:1497-1500.
6. Pao W, Miller V, Zakowski M, Doherty J, Politi K, Sarkaria I, et al. EGF receptor gene mutations are common in lung cancers from "never smokers" and are associated with sensitivity of tumors to gefitinib and erlotinib. Proceedings of the National Academy of Sciences of the United States of America. 2004;101:13306-13311.
7. Maemondo M, Inoue A, Kobayashi K, Sugawara S, Oizumi S, Isobe H, et al. Gefitinib or chemotherapy for non-small-cell lung cancer with mutated EGFR. N Engl J Med. 2010;362:2380-2388.
8. Mok T S, Cheng Y, Zhou X, Lee K H, Nakagawa K, Niho S, et al. Improvement in Overall Survival in a Randomized Study That Compared Dacomitinib With Gefitinib in Patients With Advanced Non-Small-Cell Lung Cancer and EGFR-Activating Mutations. J Clin Oncol. 2018;36:2244-2250.
9. Popat S. Osimertinib as First-Line Treatment in EGFR-Mutated Non-Small-Cell Lung Cancer. N Engl J Med. 2018;378:192-193.
10. Takano T, Ohe Y, Sakamoto H, Tsuta K, Matsuno Y, Tateishi U, et al. Epidermal growth factor receptor gene mutations and increased copy numbers predict gefitinib sensitivity in patients with recurrent non-small-cell lung cancer. J Clin Oncol. 2005;23:6829-6837.
11. Bell D W, Lynch T J, Haserlat S M, Harris P L, Okimoto R A, Brannigan B W, et al. Epidermal growth factor receptor mutations and gene amplification in non-small-cell lung cancer: molecular analysis of the IDEAL/INTACT gefitinib trials. J Clin Oncol. 2005;23:8081-8092.
12. Han S-W, Kim T-Y, Hwang P G, Jeong S, Kim J, Choi I S, et al. Predictive and Prognostic Impact of Epidermal Growth Factor Receptor Mutation in Non–Small-Cell Lung Cancer Patients Treated With Gefitinib. Journal of Clinical Oncology. 2005;23:2493-2501.
13. Fan X, Furnari F B, Cavenee W K, Castresana J S. Non-isotopic silver-stained SSCP is more sensitive than automated direct sequencing for the detection of PTEN mutations in a mixture of DNA extracted from normal and tumor cells. Int J Oncol. 2001;18:1023-1026.
14. Kimura H, Kasahara K, Kawaishi M, Kunitoh H, Tamura T, Holloway B, et al. Detection of Epidermal Growth Factor Receptor Mutations in Serum as a Predictor of the Response to Gefitinib in Patients with Non–Small-Cell Lung Cancer. Clinical Cancer Research. 2006;12:3915.
15. Kimura H, Suminoe M, Kasahara K, Sone T, Araya T, Tamori S, et al. Evaluation of epidermal growth factor receptor mutation status in serum DNA as a predictor of response to gefitinib (IRESSA). British journal of cancer. 2007;97:778-784.
16. Thomas R K, Nickerson E, Simons J F, Jänne P A, Tengs T, Yuza Y, et al. Sensitive mutation detection in heterogeneous cancer specimens by massively parallel picoliter reactor sequencing. Nat Med. 2006;12:852-855.
17. Yoshikawa S, Kukimoto-Niino M, Parker L, Handa N, Terada T, Fujimoto T, et al. Structural basis for the altered drug sensitivities of non-small cell lung cancer-associated mutants of human epidermal growth factor receptor. Oncogene. 2013;32:27-38.

18. Group T d, Huggett J F. The Digital MIQE Guidelines Update: Minimum Information for Publication of Quantitative Digital PCR Experiments for 2020. Clinical Chemistry. 2020;66:1012-1029.
19. Whale A S, Bushell C A, Grant P R, Cowen S, Gutierrez-Aguirre I, O'Sullivan D M, et al. Detection of Rare Drug Resistance Mutations by Digital PCR in a Human Influenza A Virus Model System and Clinical Samples. J Clin Microbiol. 2016;54:392-400.
20. Pholwat S, Stroup S, Foongladda S, Houpt E. Digital PCR to detect and quantify heteroresistance in drug resistant Mycobacterium tuberculosis. PLoS One. 2013;8:e57238.
21. Macher H C, García-Fernández N, Adsuar-Gómez A, Porras-López M, González-Calle A, Noval-Padillo J, et al. Donor-specific circulating cell free DNA as a noninvasive biomarker of graft injury in heart transplantation. Clin Chim Acta. 2019;495:590-597.
22. Beck J, Oellerich M, Schütz E. A Universal Droplet Digital PCR Approach for Monitoring of Graft Health After Transplantation Using a Preselected SNP Set. Methods Mol Biol. 2018;1768:335-348.
23. Chang M Y, Ahn S, Kim M Y, Han J H, Park H R, Seo H K. One-step noninvasive prenatal testing (NIPT) for autosomal recessive homozygous point mutations using digital PCR. 2018;8:2877.
24. Pekin D, Skhiri Y, Baret J C, Le Corre D, Mazutis L, Salem C B, et al. Quantitative and sensitive detection of rare mutations using droplet-based microfluidics. Lab Chip. 2011;11:2156-2166.
25. Svec D, Tichopad A, Novosadova V, Pfaffl M W, Kubista M. How good is a PCR efficiency estimate: Recommendations for precise and robust qPCR efficiency assessments. Biomol Detect Quantif. 2015;3:9-16.
26. Huggett J F, Foy C A, Benes V, Emslie K, Garson J A, Haynes R, et al. The digital MIQE guidelines: Minimum Information for Publication of Quantitative Digital PCR Experiments. Clin Chem. 2013;59:892-902.
27. Ning Y, Cui X, Yang C, Jing F, Bian X, Yi L, et al. A self-digitization chip integrated with hydration layer for low-cost and robust digital PCR. Anal Chim Acta. 2019;1055:65-73.
28. Cui X, Wu L, Wu Y, Zhang J, Zhao Q, Jing F, et al. Fast and robust sample self-digitization for digital PCR. Anal Chim Acta. 2020;1107:127-134.

Figures

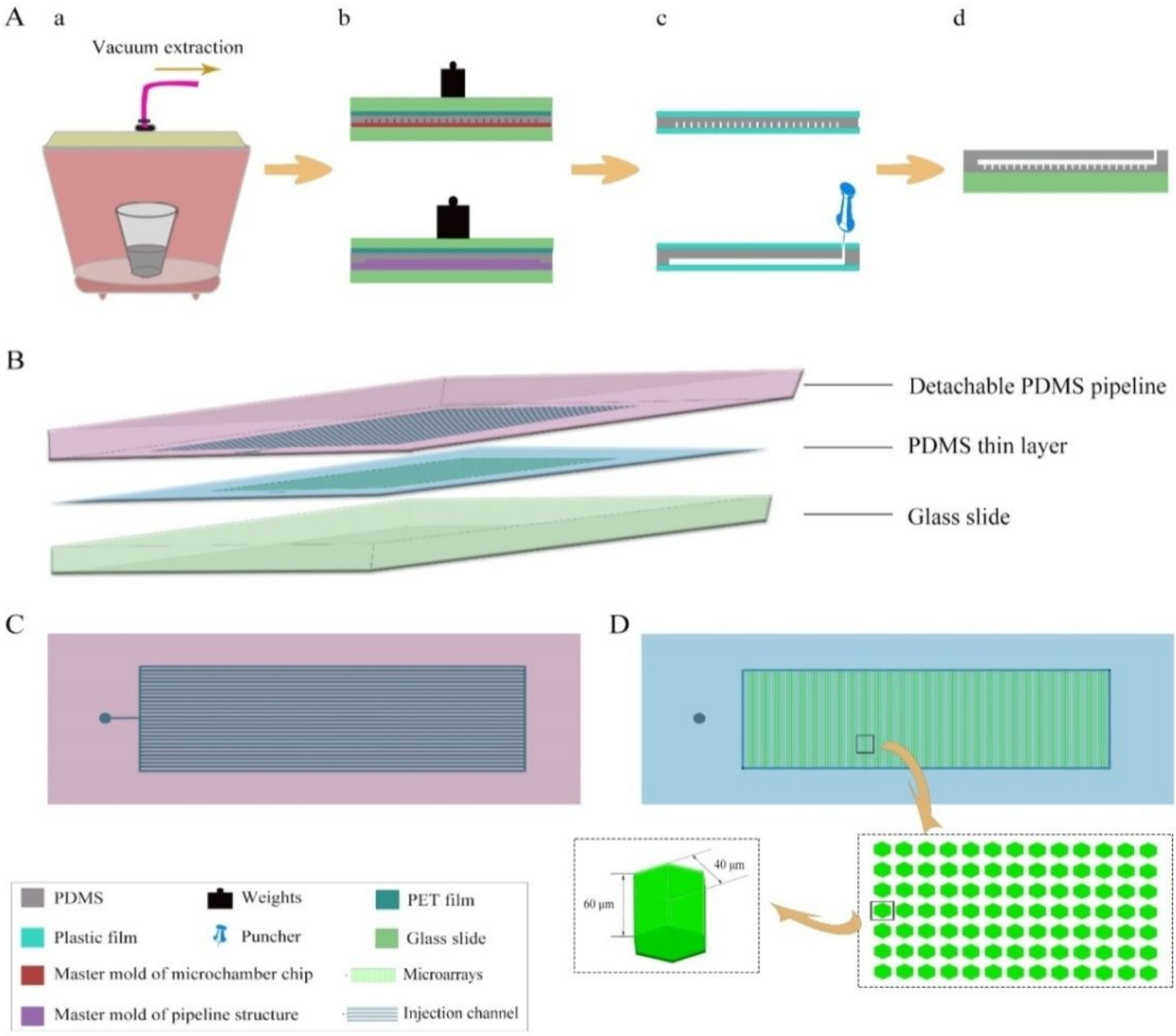

Figure 1

A: Diagram of chip preparation. B: Explosive view of LHMC. C: Top view of the PDMS pipeline. D: Top view of the PDMS thin layer.

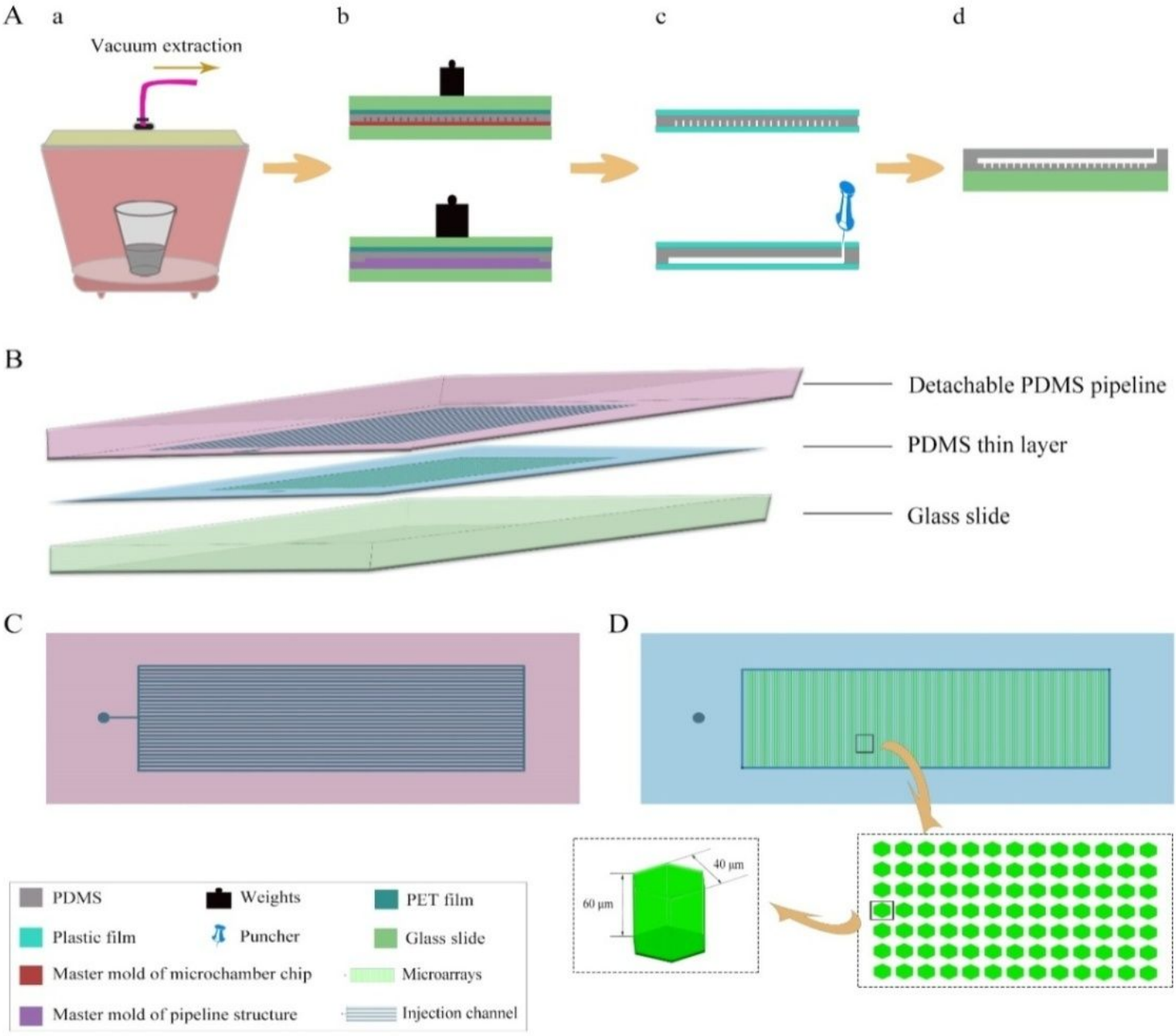

Figure 1

A: Diagram of chip preparation. B: Explosive view of LHMC. C: Top view of the PDMS pipeline. D: Top view of the PDMS thin layer.

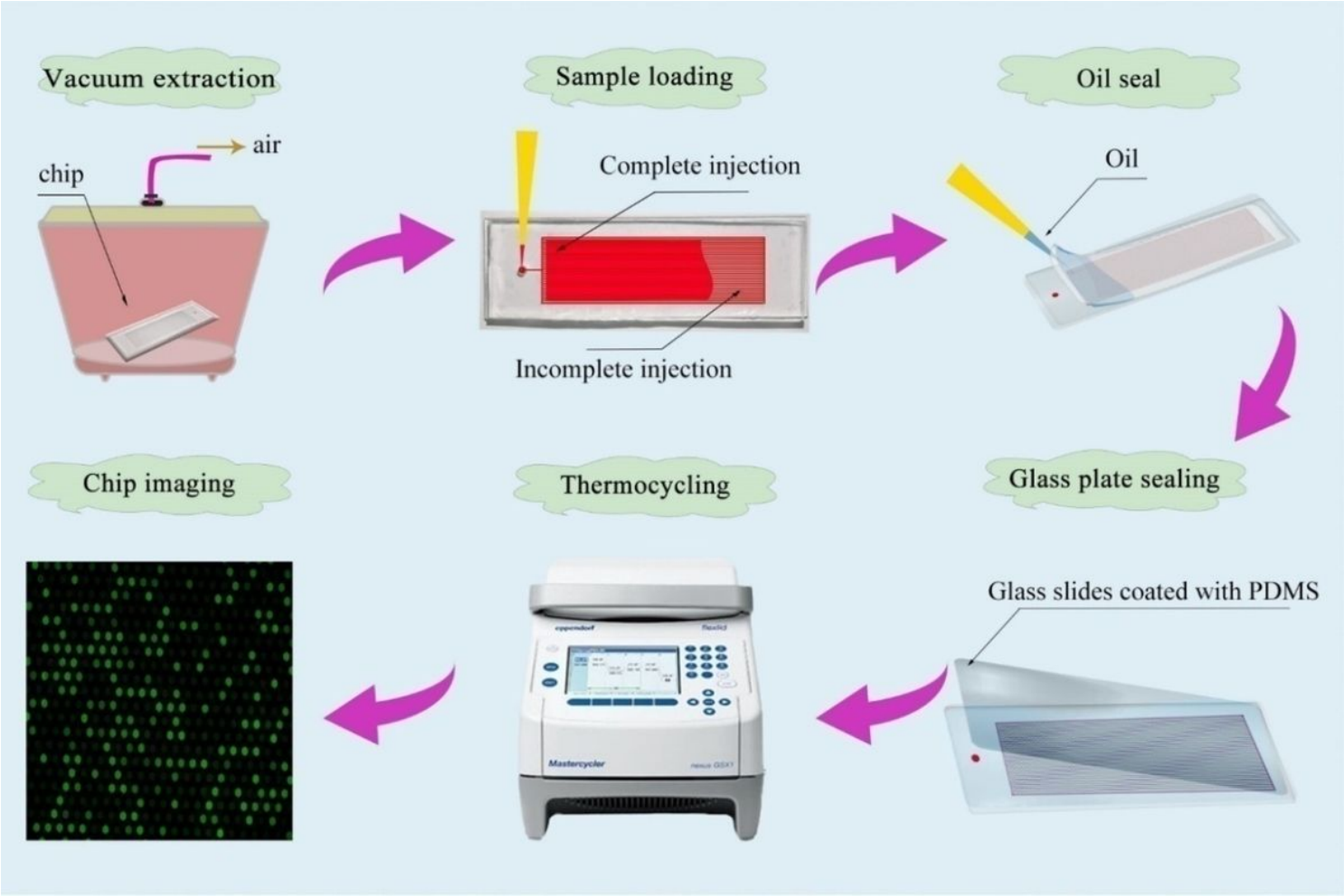

Figure 2

Schematic diagram of the LHMC-dPCR detection

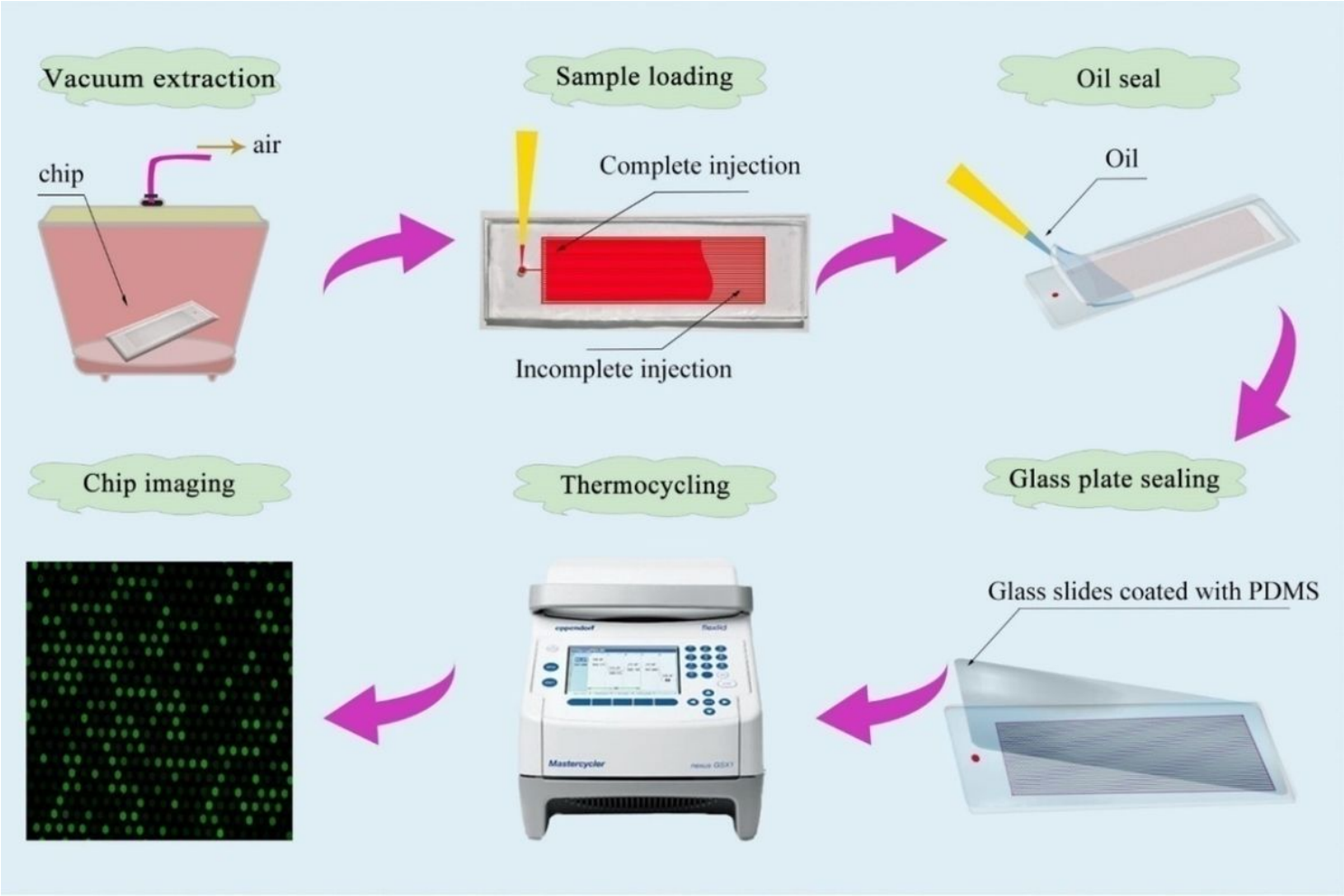

Figure 2

Schematic diagram of the LHMC-dPCR detection

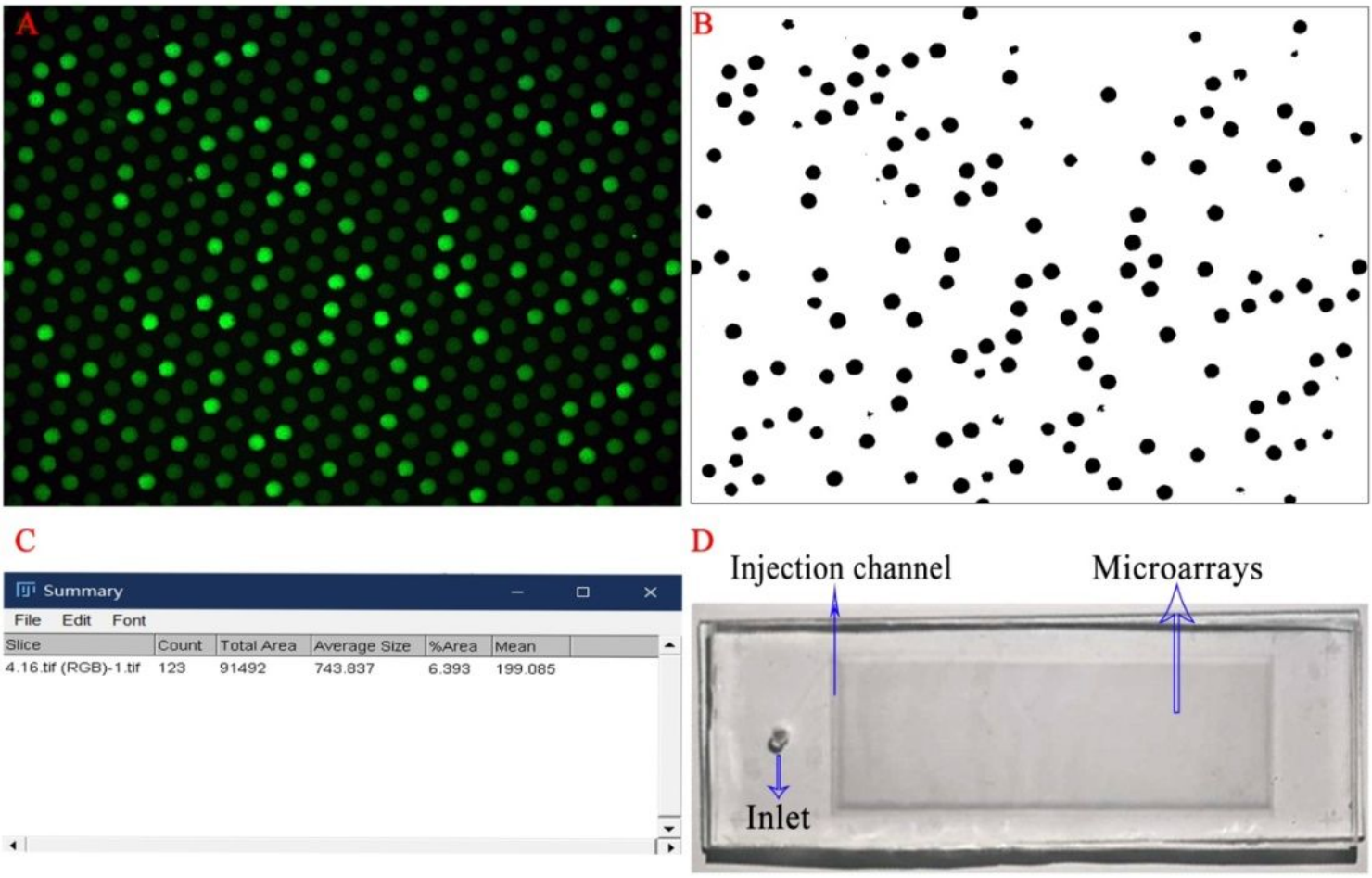

Figure 3

Diagram of fluorescence counting and physical image of the LHMC. A: Fluorescence image of the chip under the microscope. B: Grayscale image of fluorescence image processed by ImageJ. C: Figure of statistical results by ImageJ. D: The physical image of the LHMC.

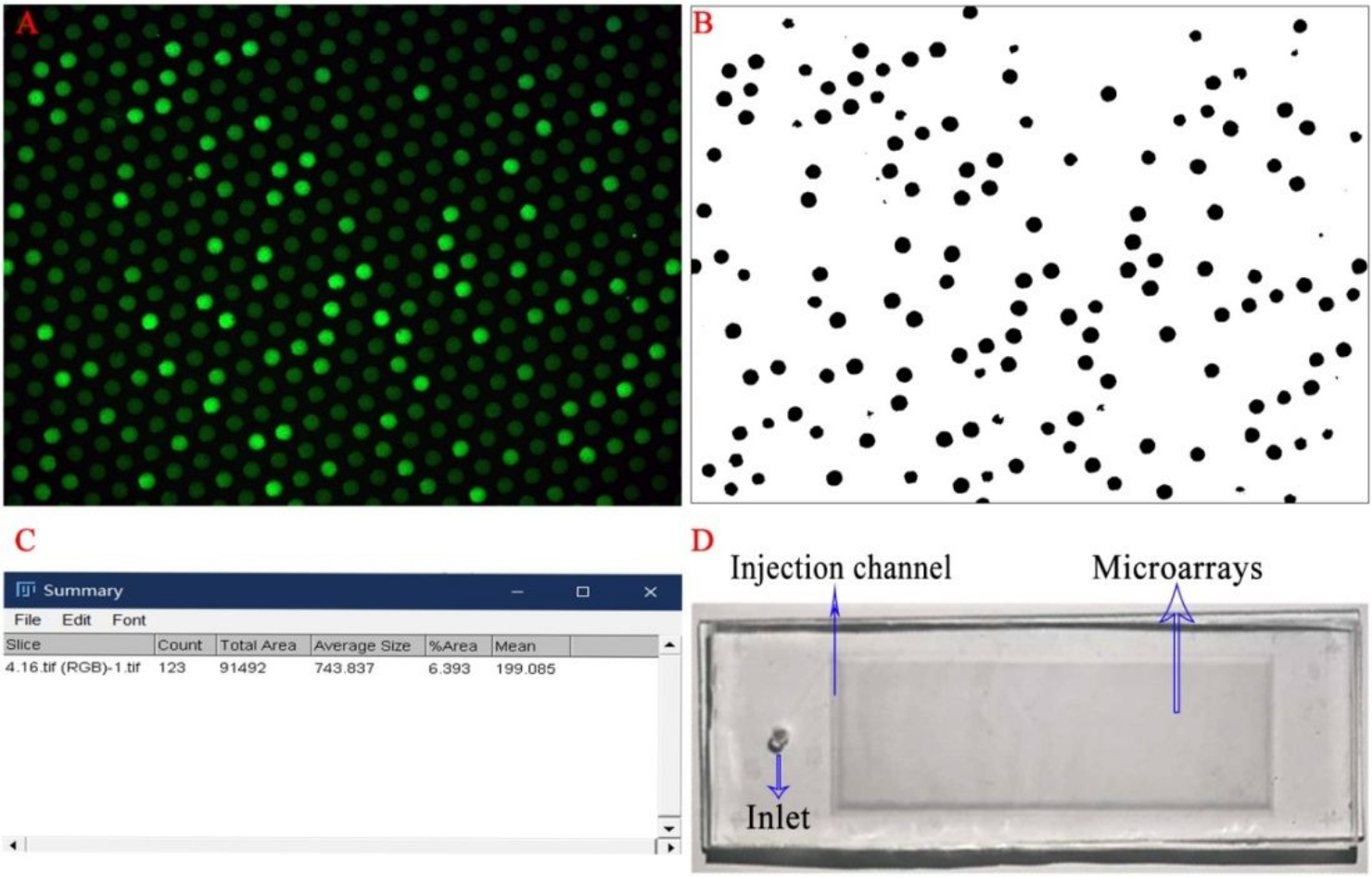

Figure 3

Diagram of fluorescence counting and physical image of the LHMC. A: Fluorescence image of the chip under the microscope. B: Grayscale image of fluorescence image processed by ImageJ. C: Figure of statistical results by ImageJ. D: The physical image of the LHMC.

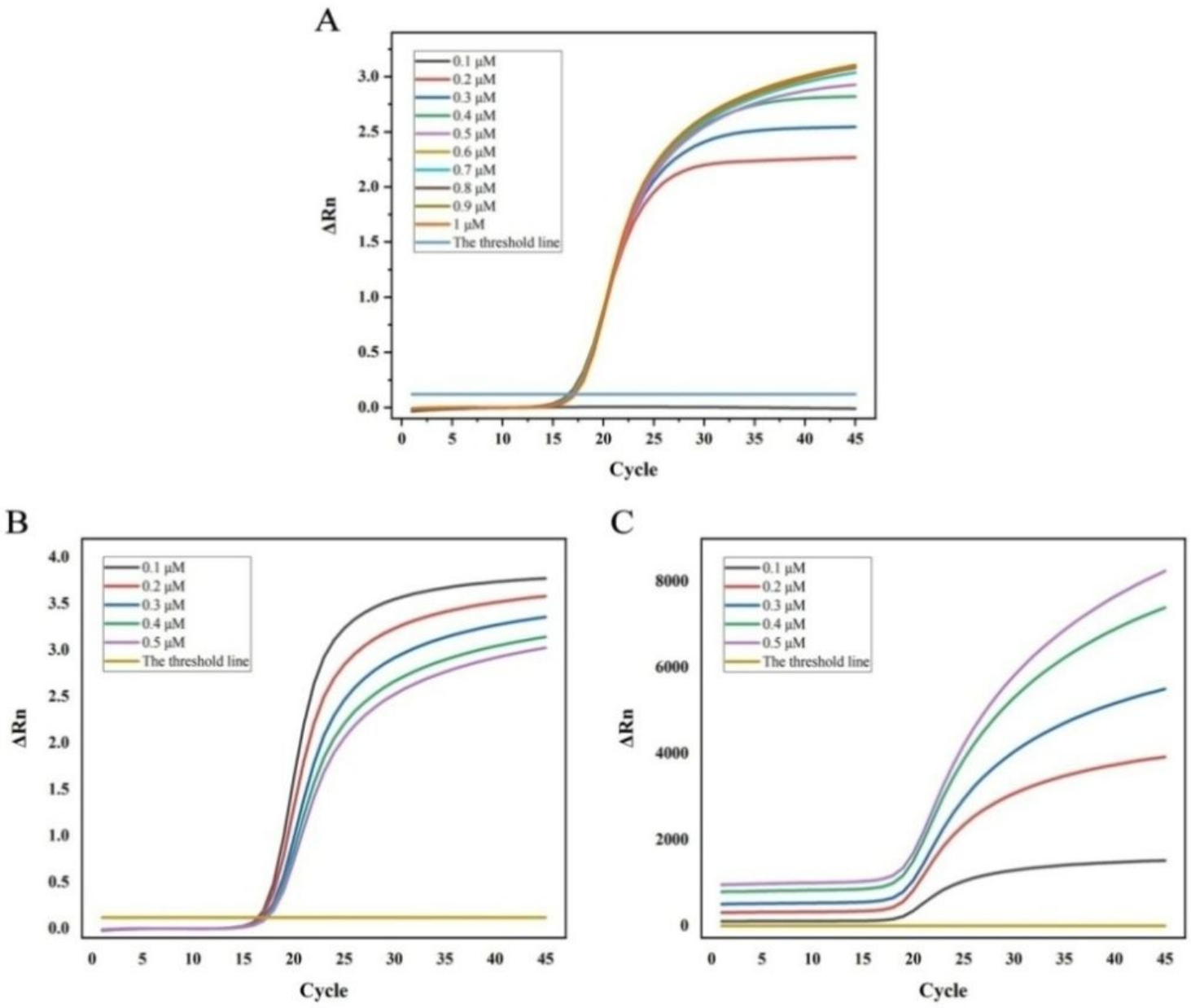

Figure 4

The graphs of optimized primer and probe concentration. A: The amplification curve with optimized primer concentration. B: The amplification curve with optimized probe concentration. C: The original curve with optimized probe concentration.

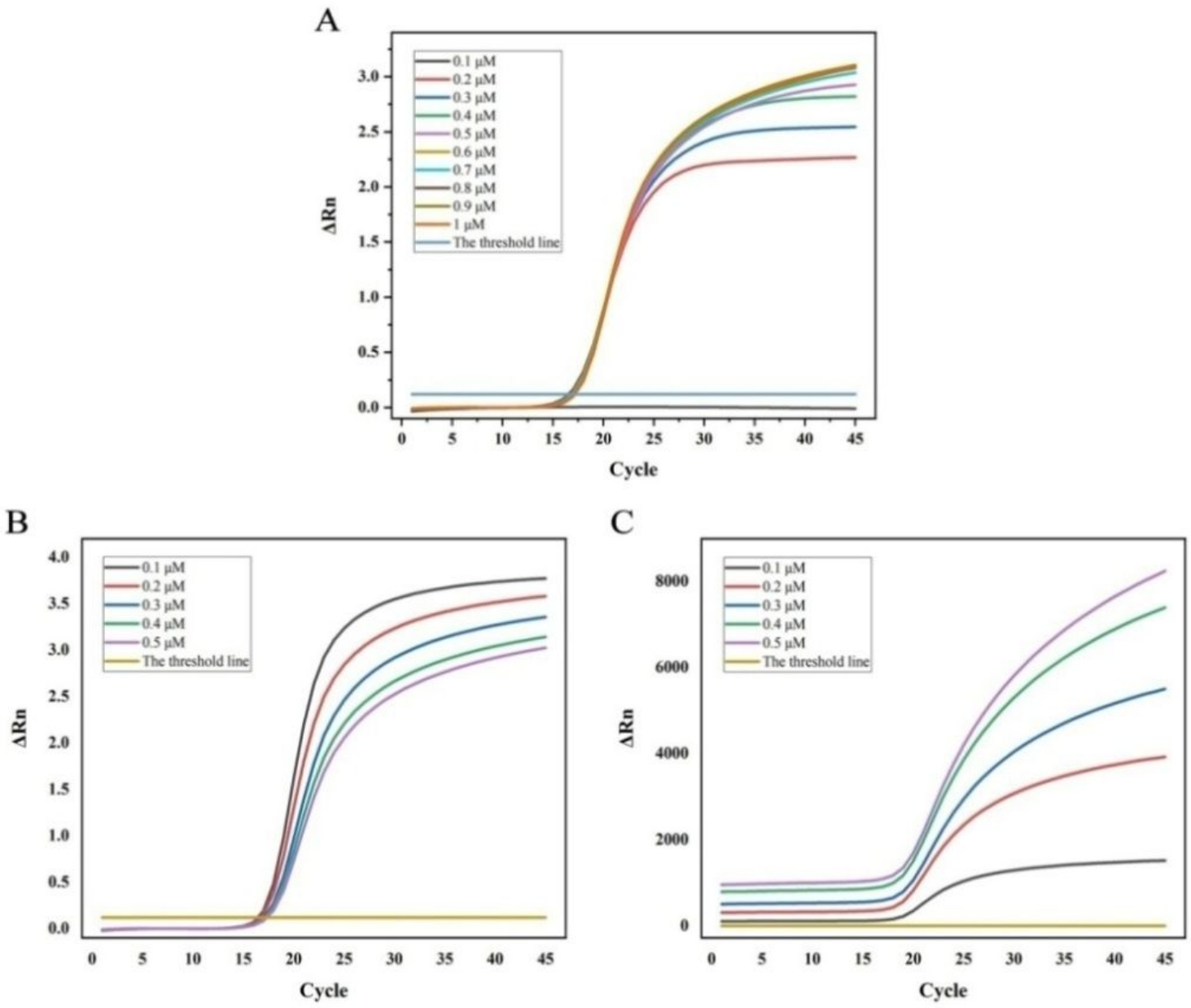

Figure 4

The graphs of optimized primer and probe concentration. A: The amplification curve with optimized primer concentration. B: The amplification curve with optimized probe concentration. C: The original curve with optimized probe concentration.

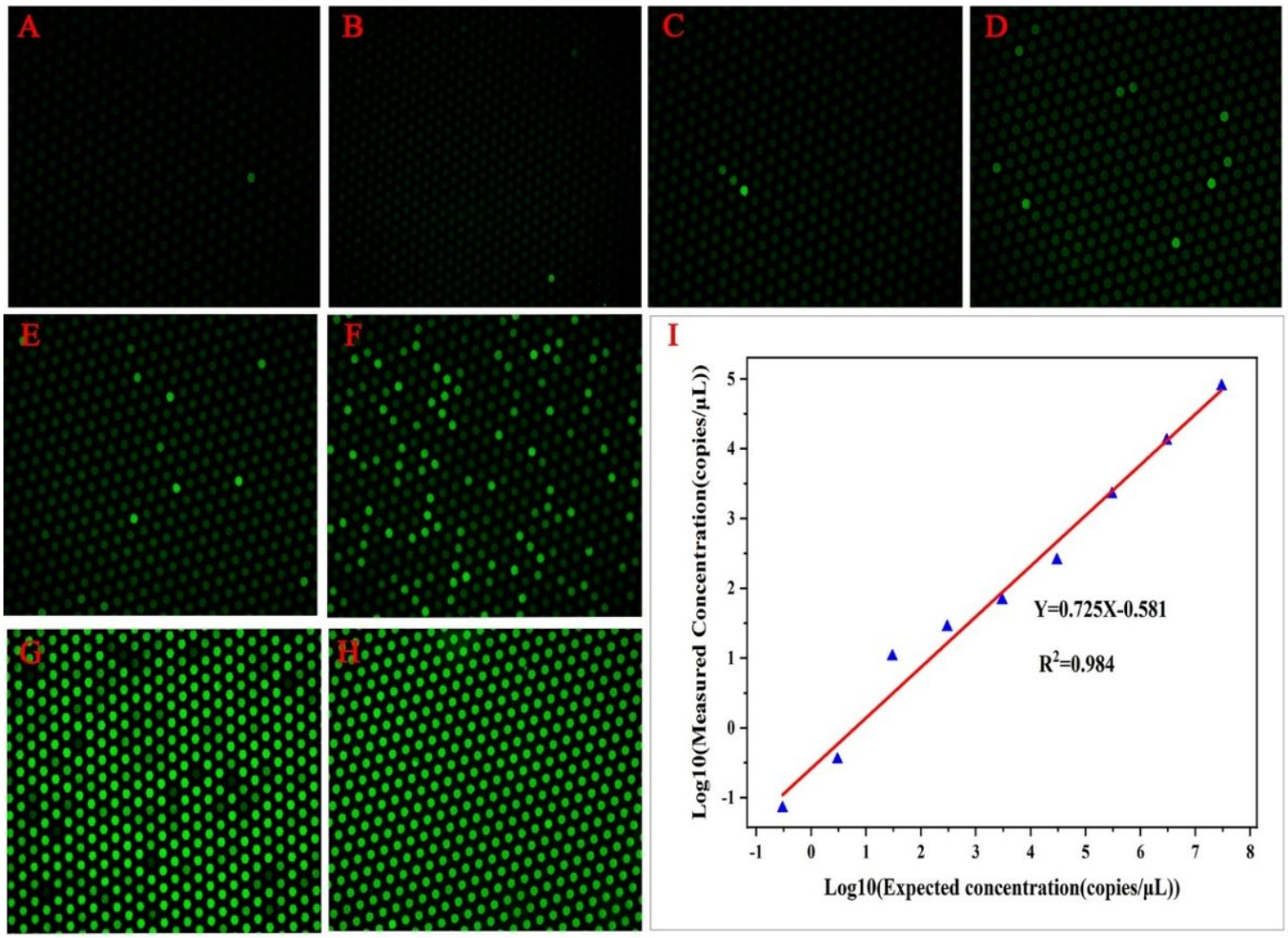

Figure 5

The fluorescence and linear graphs of 8 mutant plasmids with 10-fold gradient concentration. A-H: The fluorescence microscopy of standard plasmids No. 1-8 in sequence. I: The linear relationship between the measured value (copies/μL) in the LHMC and the expected one (copies/μL).

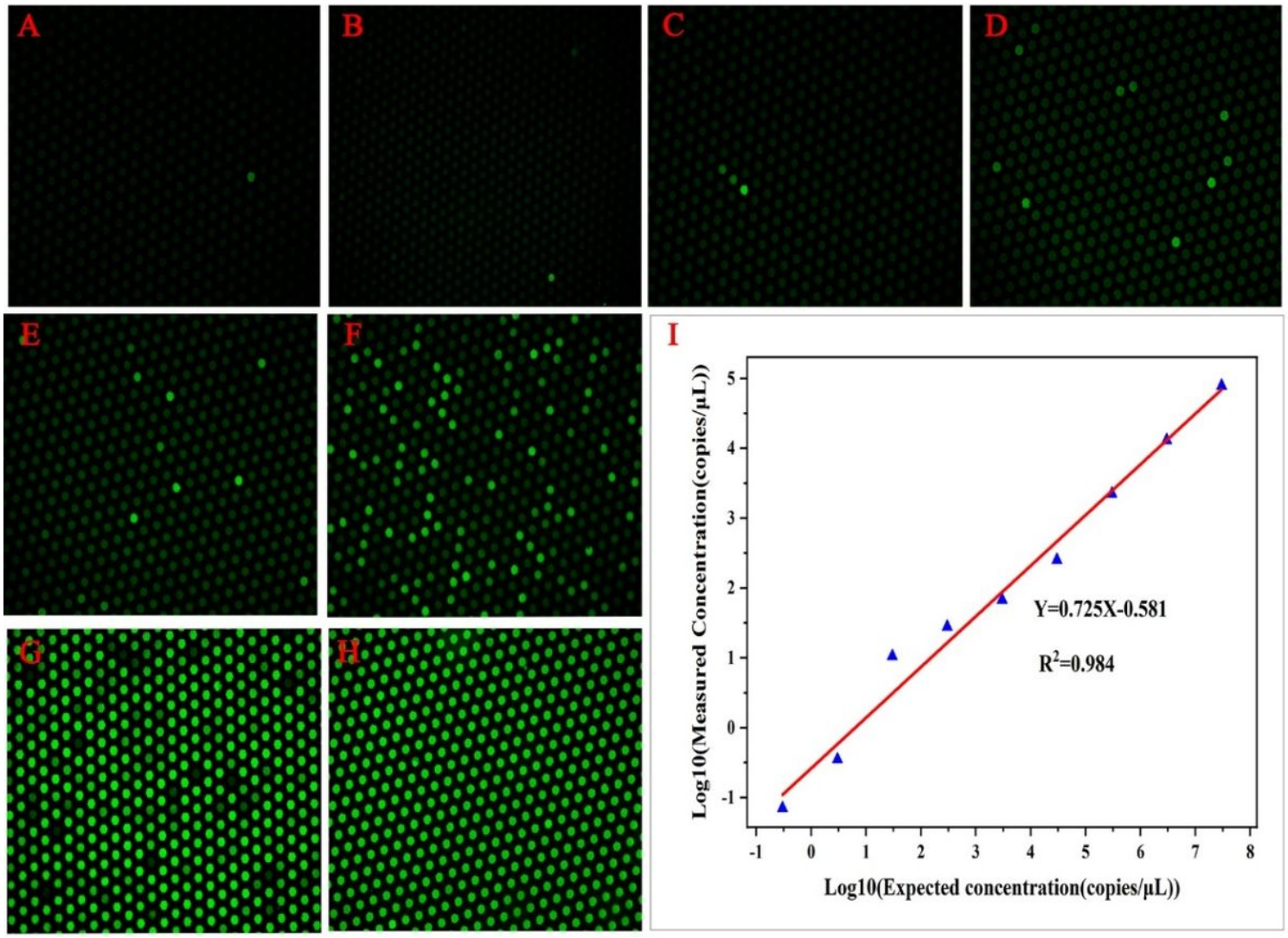

Figure 5

The fluorescence and linear graphs of 8 mutant plasmids with 10-fold gradient concentration. A-H: The fluorescence microscopy of standard plasmids No. 1-8 in sequence. I: The linear relationship between the measured value (copies/μL) in the LHMC and the expected one (copies/μL).

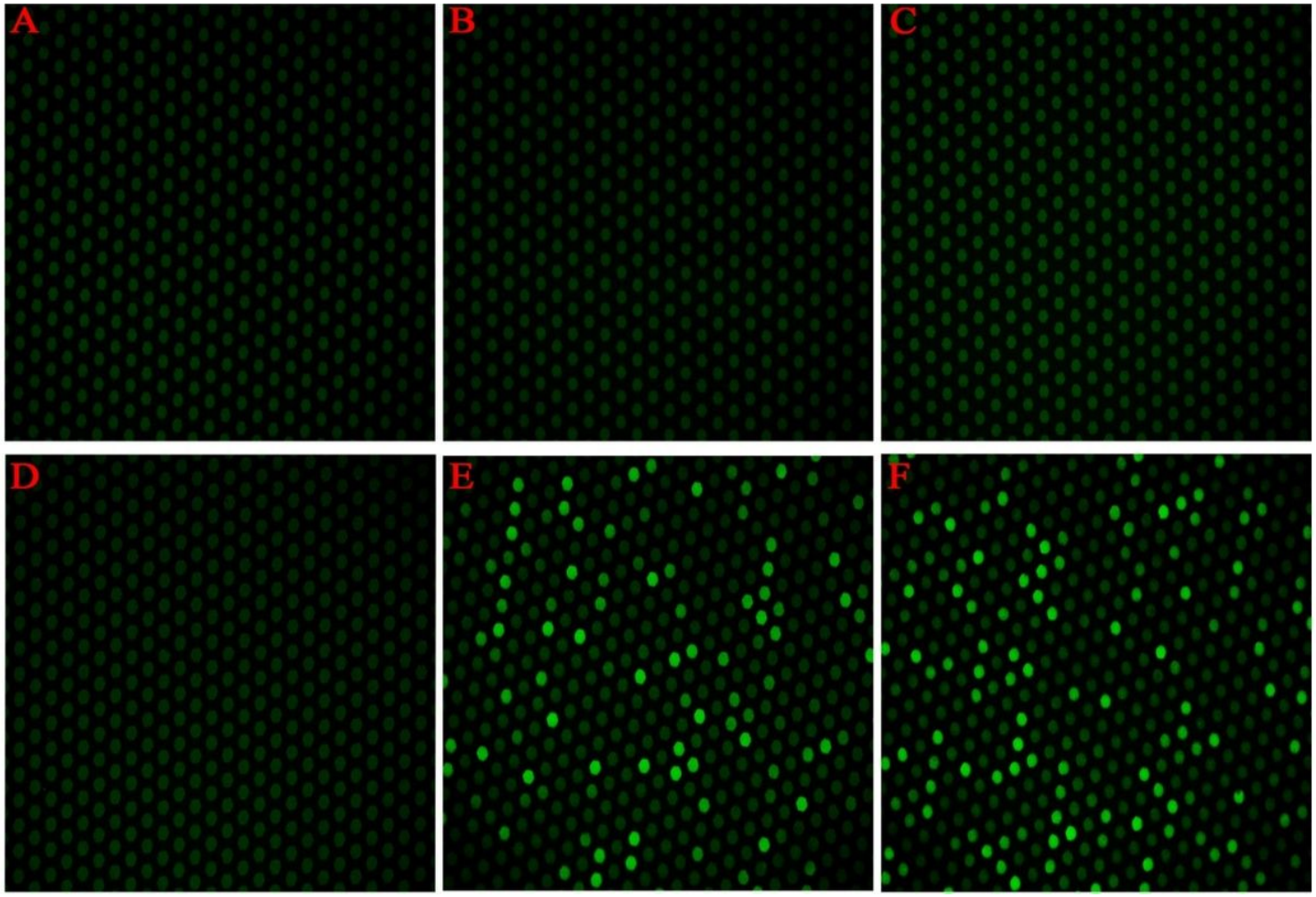

Figure 6

Fluorescence microscope image of specificity analysis. A: 20.5 g/L albumin standard solution; B: 3.01×108 copies/μL Codon12 mutant plasmids; C: 3.20×108 copies/μL L858R mutant plasmids; D: 2.88×108 copies/μL H19-1 mutant plasmids; E: The mixture of the above interfering substances and 3.01×105 copies/μL G719S mutant plasmids; F: The similarly diluted standard No. 6.

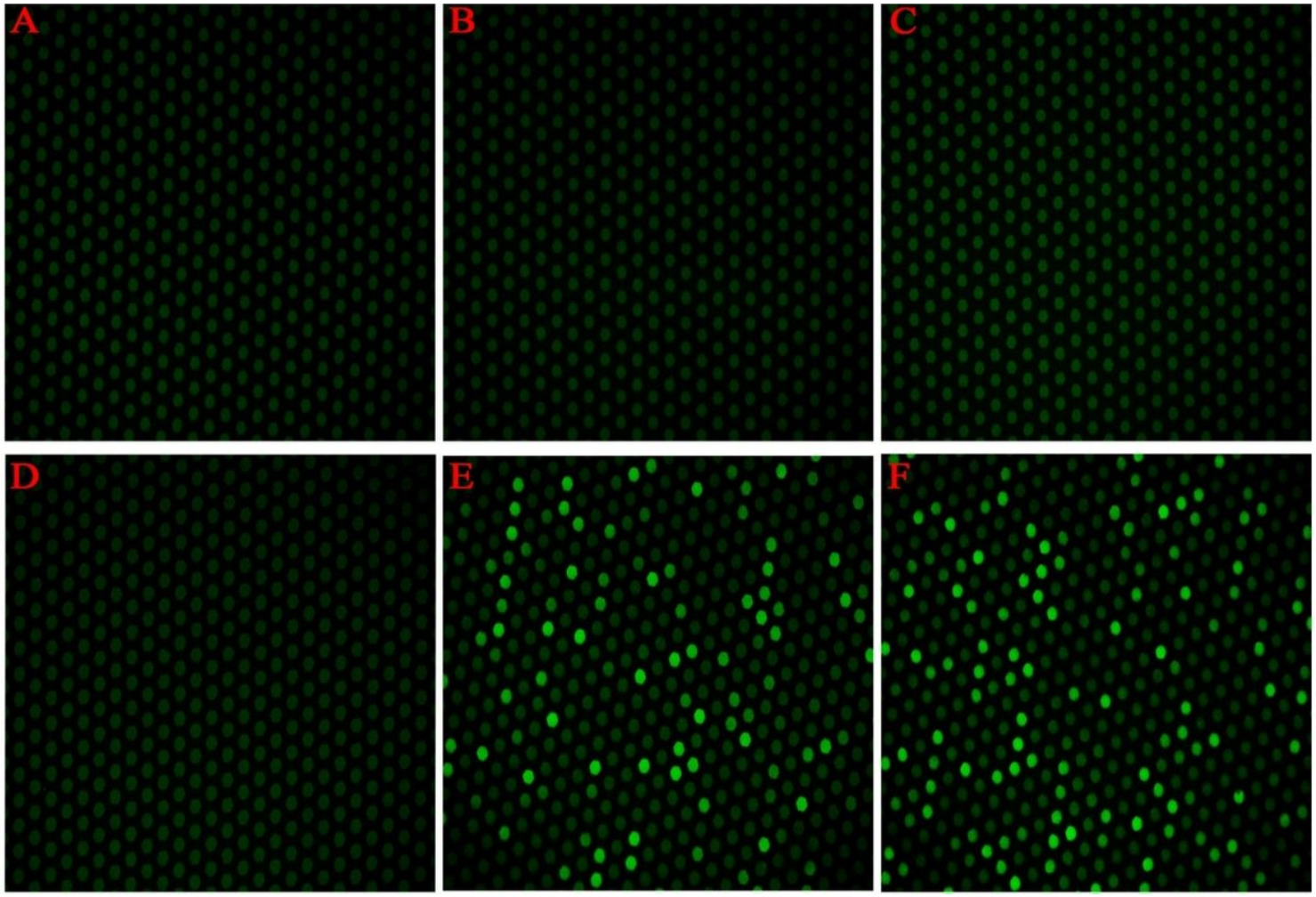

Figure 6

Fluorescence microscope image of specificity analysis. A: 20.5 g/L albumin standard solution; B: 3.01×108 copies/μL Codon12 mutant plasmids; C: 3.20×108 copies/μL L858R mutant plasmids; D: 2.88×108 copies/μL H19-1 mutant plasmids; E: The mixture of the above interfering substances and 3.01×105 copies/μL G719S mutant plasmids; F: The similarly diluted standard No. 6.

Supplementary Files

This is a list of supplementary files associated with this preprint. Click to download.

- 2SupplementaryResults.docx
- 2SupplementaryResults.docx